doi:10.3772/j.issn.1006-6748.2020.03.002

A novel flow control scheme for reciprocating compressor based on adaptive predictive PID control①

Liu Wenhua (刘雯华)*, Zhang Jinjie②*, Zhou Chao*, Wang Yao*, Sun Xu**, Hong Huaibing**
(*Compressor Health and Intelligent Monitoring Center of National Key Laboratory of Compressor Technology, Beijing University of Chemical Technology, Beijing 100029, P. R. China)
(**Beijing Key Laboratory of Health Monitoring Control and Fault Self-Recovery for High-End Machinery, Beijing University of Chemical Technology, Beijing 100029, P. R. China)

Abstract

In the process of capacity regulation of reciprocating compressor, the frequent change of inlet temperature and pressure makes the control of exhaust flow unstable, resulting in the high pressure ratio of the intermediate stage. At last the compressor cannot operate safely. To solve the problem, a novel flow control scheme based on inlet temperature and pressure ratio is proposed. In this scheme, the intake model of the cylinder under the capacity regulation condition is established to calculate the load of the first cylinder. Then, the adaptive predictive PID (APPID) controller is designed to control the pressure ratio of other stages, and the grey prediction model is used to predict the pressure output to overcome the system delay. To solve the problem of control parameters tuning, an improved particle swarm optimization (PSO) algorithm is adopted to obtain the optimal control parameters. The effectiveness of the adaptive predictive PID control method is verified by a two-stage compressor model simulation. Finally, the flow control scheme is applied to the actual four-stage air reciprocating compressor flow control system. Although the temperature difference is greater than 15 ℃, the compressor exhaust flow is maintained at the set value and the pressure ratio is also maintained stable. At the same time, the compressor pressure ratio can be quickly adjusted without overshoot. The application result further verifies the feasibility and effectiveness of the scheme.

Key words: reciprocating compressor, capacity control, predictive PID control, internal model control (IMC)

0 Introduction

Reciprocating compressors are key equipment most commonly used in oil extraction, gas production, oil refining, chemical industries, refrigeration, and gas transmission[1]. But, in practice, excess gas is compressed repeatedly resulting in a large amount of energy waste since the capacity of the compressor is usually regulated by backflow. To solve the high energy waste problem of reciprocating compressor, many capacity regulation methods for reciprocating compressors have been developed, including intermittent operation of compressor, suction-gas throttling scheme, cylinder unloading scheme and jacking suction valve backflow scheme[2-4]. With the advantages of wide adjustable range and high energy saving, the method by controlling suction valve has become the most popular method to solve the high energy consumption of reciprocating compressor[5,6].

The control nature of the exhaust flow regulation of the reciprocating compressor belongs to pressure control. Since reciprocating compressor is usually a two-stage compressor or more, the whole pressure control has strong coupling and nonlinearity. However, the operating condition of the compressor requires that the pressure of the buffer tank should not fluctuate greatly during the flow regulation process, which is a great challenge to the pressure control of the system with strong coupling and nonlinearity. Wang et al.[7] designed a set of compressor capacity control system by using s7-300 series programmable logic controller, the exhaust pressure of each stage of the compressor was controlled by the method of recursive refluxing step by

① Supported by the State Key Laboratory of Compressor Technology Open Fund Project (No. SKLYSJ201808/SKLYS201811) and the National Key Research and Development Plan (No. 2016YFF0203305).
② To whom correspondence should be addressed. E-mail: zjj87427@163.com
Received on Dec. 24, 2019

step, and the load of each stage was automatically calculated by PID controller. Refs[8,9] also used PI controllers to control pressure. However, due to the coupling effect between different stages, the controlling overshoot led to obvious pressure fluctuation, and the regulation effects were not satisfactory. In Ref. [10], the internal model controller was used instead of traditional PID controller to optimize the control effect of flow regulation of two-stage reciprocating compressor, which achieved good performance. However, the accurate modeling of the compressor was required, and the settling time was long.

In most applications, considering the process stability or limited hardware conditions, the manual mode, that is, setting exhaust flow manually is used for flow control. In this mode, it is necessary to constantly adjust the set exhaust flow rate, due to the change of the inlet temperature, pressure and other operating conditions. To solve this issue, a novel compressor flow control scheme based on intake temperature and pressure ratio is proposed. Firstly, the cylinder intake model under the capacity regulation condition is established to calculate the load of the 1st stage cylinder at different intake temperatures. Secondly, the pressure ratio of each stage of the compressor is controlled by predictive PID controller.

To solve the problem of coupling relationship between different stages, the multivariable grey prediction model is used. The deviation between the predicted value and the set value is input into the PID controller for automatic load calculation to ensure the rapidity and stability of pressure control. Furthermore, the adaptive proportion coefficient is introduced to prevent the deterioration of control performance due to the decrease of prediction model accuracy. It is not easy to find a set of PID control parameter to coordinate the rapidity, overshoot and steady error of the system. Therefore, an improved particle swarm optimization algorithm is adopted to obtain the optimal control parameters.

This paper is organized as follows. Section 1 introduces the composition and working principle of the stepless capacity regulation system. Section 2 describes a novel flow control scheme. The comparison of simulation results among adaptive predictive PID (APPID) control with traditional PID control and internal model control is analyzed in Section 3. Section 4 introduces the application case of the control scheme proposed in this study. Finally, Section 5 concludes the work.

1 System composition and principle of regulation

The stepless capacity regulation system (SCRS) for reciprocating compressor is mainly composed of hydraulic mechanism, actuator and control unit. The hydraulic mechanism includes hydraulic oil station, accumulator, high-speed solenoid valve, hydraulic pipeline, etc., to provide the required oil pressure for the actuator. The actuator is composed of compressor suction valve, actuating cylinder and unloader. The control unit includes controller, solenoid valve drive module, upper computer and so on. The structure diagram of a two-stage reciprocating compressor equipped with SCRS is shown in Fig. 1.

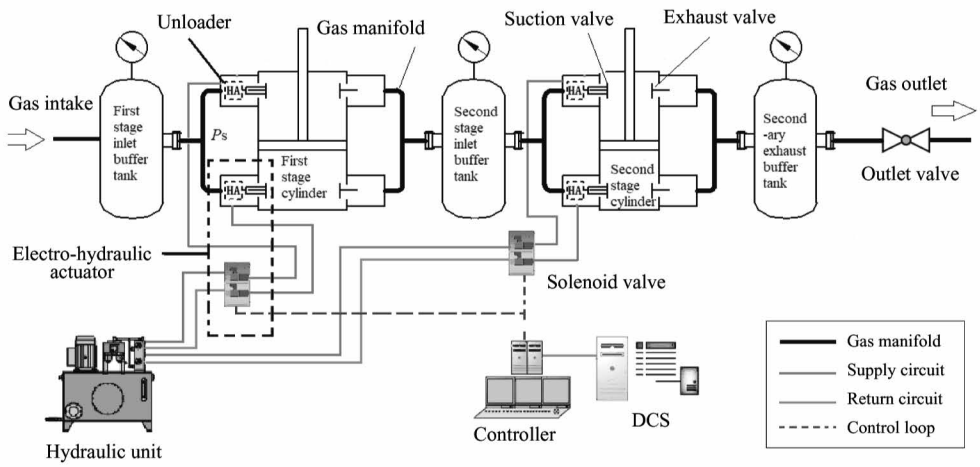

Fig. 1 Composition of stepless capacity regulation system

The actuator driven by the hydraulic pressure control the opening and delayed closing of inlet valve to regulate the exhaust flow. Therefore, SCRS makes a new backflow process in addition to the original work

cycle. By controlling the duration of the backflow process accurately, the accurate control of different exhaust flow can be achieved. The working principle of the system is shown in Fig. 2.

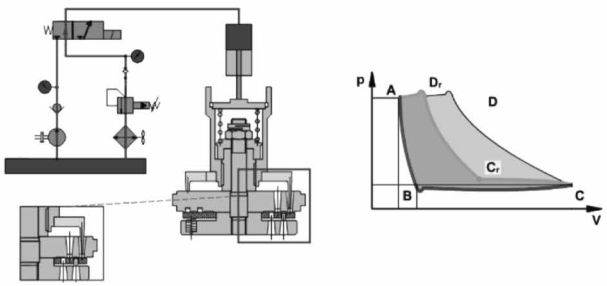

Fig. 2 Schematic diagram of SCRS

The working cycle of the reciprocating compressor under the capacity regulation condition includes the following 5 processes.

1) Expansion process: curve A-B. The pressure of the high pressure gas remaining in the cylinder clearance gradually decreases after expansion, and the inlet and exhaust valves are closed.

2) Suction process: curve B-C. When the pressure in the cylinder is lower than a certain value, the inlet valve opens automatically under the action of pressure difference, and the suction process ends at point C.

3) Backflow process: curve C-Cr. At point C, the high speed solenoid valve is energized, and the suction valve is forced to open by the actuator driven by high hydraulic oil and remains open. The air being sucked into the cylinder is returned to the intake line without compressed through the jacked suction valve.

4) Compression process: curve Cr-Dr. At the end of the backflow process, that is, at the point Dr, the high-speed solenoid valve is cut off, the actuator is withdrawn under the action of the unloader spring, and the suction valve is closed under the action of the pressure difference, and then the compressor enters the compression process.

5) Exhaust process: curve Dr-A. The exhaust valve opens automatically under the action of differential pressure when the pressure in the cylinder is higher than a certain value. The compressor enters the exhaust process.

Through the above new working cycle, the excess capacity is returned to the inlet pipe through the inlet valve and no energy is wasted. Thus, it can be seen that the area of the dynamic pressure indicator diagram of the compressor decreases significantly (as shown in Fig. 2) and the power decreases.

In addition, the main control objective of the SCRS is to ensure that the pressure of each stage exhaust buffer tank can quickly track the set value and remain stable under disturbance by controlling the load of the front and rear cylinder of the buffer tank.

2 Flow control scheme

To regulate the capacity of the compressor, it is necessary to adjust the pressure ratio of each stage of the compressor. The proper pressure ratios enable the compressor to work with best efficiency, which not only reduces the energy waste of the compressor, but also ensures the safety and stability of the compressor. Therefore, the novel flow control scheme based on intake temperature and pressure ratio is proposed.

2.1 The first stage load calculation method

The total inlet flow of the compressor varies with the inlet temperature and pressure. Therefore, a novel load calculation method is adopted to calculate the compressor inlet load (1st stage load). The 1st stage load is the ratio of the actual required exhaust flow to the current full load suction flow (standard condition).

The narrow channel flow model is applied to calculate compressor inlet flow. The mass flow equation of the gas with adiabatic flow in the narrow channel is as follows[11]:

$$\frac{\mathrm{d}m}{\mathrm{d}t} = \frac{\alpha A}{\nu}\sqrt{\frac{2k}{k-1}R_g T_{in}\left[1-\left(\frac{P_{out}}{P_{in}}\right)^{\frac{k-1}{k}}\right]} \tag{1}$$

where, m represents the mass of the gas, α represents the flow coefficient, A represents the channel area, k is the specific heat ratio, ν is the specific volume of the gas in the cylinder, T_{in} is the gas temperature of the tight narrow passage, R_g is the general gas constant, P_{in} and P_{out} represents the pressure of the gas flowing in and out of the narrow passage, respectively.

According to the working principle of the compressor, the pressure in the cylinder during the suction process of the compressor can be expressed as[12]

$$\frac{\mathrm{d}P_{cy}}{\mathrm{d}\theta} = -\frac{1}{\omega}\left\{\begin{aligned}&\frac{kP_{cy}}{V_{1cy}}\frac{\mathrm{d}V_{cy}}{\mathrm{d}\theta} - k\frac{\alpha_{sv}A_{sv}}{V_{1cy}}\times\\&P_1\left(\frac{P_{cy}}{P_1}\right)^{\frac{1}{k}}\sqrt{\frac{2k}{k-1}R_g T_s\left[1-\left(\frac{P_{cy}}{P_1}\right)^{\frac{k-1}{k}}\right]}\end{aligned}\right\} \tag{2}$$

The real-time volume of the cylinder when the piston moves in the cylinder V_{cy} is

$$V_{cy} = \alpha_h V_h + \frac{V_h}{2}\left(1-\cos\theta+\frac{\lambda}{2}\sin^2\theta\right) \tag{3}$$

where, α_h is the clearance coefficient of the first cylinder, V_h is the piston stroke volume of cylinder, λ is the ratio of cylinder connecting rod length to crankshaft ra-

dius, V_0 is the clearance volume of cylinder.

Combined with Eq. (1) and Eq. (3), the single-cycle full-load intake capacity of the compressor can be expressed as

$$M_{1s} = \int_0^{\pi} \frac{S_1 \alpha_{sv} A_{1sv} P_{1cy} \left(\frac{P_1}{P_{1cy}}\right)^{\frac{k-1}{k}}}{\omega R_g T_{1s}} \sqrt{\frac{2k}{k-1} R_g T_{1s} \left[1 - \left(\frac{P_{1cy}}{P_1}\right)^{\frac{k-1}{k}}\right]} \mathrm{d}\theta \quad (4)$$

where, M_{1s} represents the suction mass flow of the 1st cylinder. M_{1s} is converted to standard gas volume flow rate Q_{1s}.

$$Q_{1s} = \frac{180}{\pi} \times \frac{\omega}{6} \times \frac{RT \frac{M_{1s}}{M}}{P} \quad (5)$$

where, T is absolute temperature, M is the molar mass of gas, P is the standard atmospheric pressure, ω is the compressor speed. The actual flow rate required by the production process at time t is $Q(t)$. Therefore, the load of the 1st stage cylinder of the reciprocating compressor at time t can be expressed as

$$\eta_1(t) = Q(t)/Q_{1s} \quad (6)$$

2.2 The load calculation method based on APPID

In this paper, the predictive control is combined with PID to deal with the time delay and nonlinearity of the system. The dynamic prediction model is used to solve the system's delayed deviation, and the deviation signal is sent to the controller in advance. The control signal is timely applied to the controlled object, so as to reduce overshoot and stabilize the regulation process quickly. The control flow chart is shown in Fig. 3. The grey prediction model can effectively overcome the influence of system delay by predicting the system output at the future time.

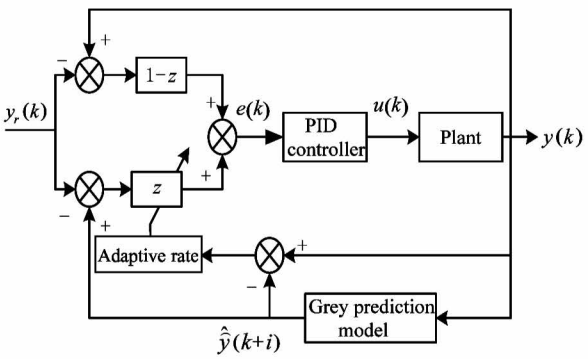

Fig. 3 Adaptive grey predictive PID control structure

2.2.1 Multivariate gray prediction model

The grey prediction model is applied to predict the pressure change in advance. There is a strong coupling relationship between each stage cylinder load and each stage buffer tank pressure. In order to solve this problem, this work transforms the multivariable system into several multi-input single output subsystems. The control problem of multivariable system is transformed into several single output subsystem control problems. For each subsystem, grey system prediction model $GM(1, N+1)$ is adopted to predict the output of the subsystem. The block diagram of grey system prediction model $GM(1, N+1)$ is shown in Fig. 4.

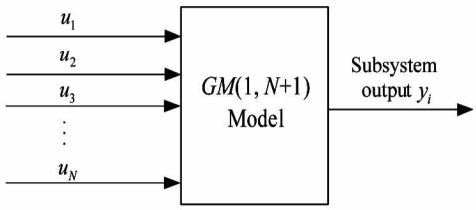

Fig. 4 $GM(1, N+1)$ block diagram of grey system prediction model

The time series of the ith subsystem of the multivariable system is as

$$U_i^{(0)} = \{u_i^{(0)}(1), u_i^{(0)}(2), \cdots, u_i^{(0)}(n)\} \quad (7)$$

$$Y_i^{(0)} = \{y_i^{(0)}(1), y_i^{(0)}(2), \cdots, y_i^{(0)}(n)\} \quad (8)$$

where, $i = 1, \cdots, N$; n represents the dimension of the data.

In order to establish the multivariable grey prediction model, the data are firstly processed and data level ratio is tested. The data level ratio is $\lambda_{ui}(t) = \frac{u_i^{(0)}(t-1)}{u_i^{(0)}(t)}$, $\lambda_{yi}(t) = \frac{y_i^{(0)}(t-1)}{y_i^{(0)}(t)}$ $(t = 2, 3, \cdots, n)$, if $\lambda_{ui}(t)$ and $\lambda_{yi}(t)$ are in the range of $(e^{-\frac{2}{N+1}}, e^{\frac{2}{N+1}})$, it can be used as the input data of $GM(1, N+1)$ model for prediction. Otherwise, the original data needs to be preprocessed.

Let $U_i^{(0)}$ and $Y_i^{(0)}$ be the primal time sequence, $U_i^{(1)}$ and $Y_i^{(1)}$ be the I-AGO (accumulated generating operation) data sequence of $U_i^{(0)}$ and $Y_i^{(0)}$, respectively. Sequence $Z_i^{(1)}$ is generated from the generated sequence adjacent to the mean value, where, $z_i^{(1)}(k) = 0.5(y_i^{(1)}(k) + y_i^{(1)}(k-1))$, $k = 2, \cdots, n$.

The gray differential equation of $GM(1, N+1)$ model can be expressed as

$$\frac{\mathrm{d}y_i^{(1)}}{\mathrm{d}t} + a_i y_i^{(1)} = \sum_{i=1}^{N} b_{ij} u_i^{(1)}(k) \quad (9)$$

where, a_i is the system development coefficient, $b_{ij}u_i^{(1)}(k)$ is the driving term and b_{ij} is the driving coefficient. $\boldsymbol{a}_i = [a_i, b_{i1}, \cdots, b_{iN}]^{\mathrm{T}}$ represents the parameter columns of the model. According to the least square method, its estimated value is

$$\hat{\boldsymbol{a}}_i = (\boldsymbol{B}_i^{\mathrm{T}} \boldsymbol{B}_i)^{-1} \boldsymbol{B}_i^{\mathrm{T}} \boldsymbol{Y}_i \quad (10)$$

where,

$$\boldsymbol{Y}_i = [y_i^{(0)}(2), y_i^{(0)}(3), \cdots, y_i^{(0)}(n)]^{\mathrm{T}} \quad (11)$$

$$\boldsymbol{B}_i = \begin{bmatrix} -z_i^{(1)}(2) & u_1^{(1)}(2) & \cdots & u_N^{(1)}(2) \\ -z_i^{(1)}(3) & u_1^{(1)}(3) & \cdots & u_N^{(1)}(3) \\ \vdots & \vdots & \ddots & \vdots \\ -z_i^{(1)}(n) & u_1^{(1)}(n) & \cdots & u_N^{(1)}(n) \end{bmatrix} \quad (12)$$

By discretizing the gray Eq. (9), the following expression can be obtained:

$$y_i^{(1)}(k+1) = (1 - Ta_i) y_i^{(1)}(k) + T \sum_{i=1}^{N} b_{ij} u_i^{(1)}(k) \quad (13)$$

where, T is the simple time. By performing I-AGO, the predicted results can be obtained as

$$y_i^{(0)}(k+1) = (1 - Ta_i) y_i^{(0)}(k) + T \sum_{i=1}^{N} b_{ij} u_i^{(0)}(k) \quad (14)$$

In the control process, the data has a certain timeliness. The parameters of the grey model are updated repeatedly to ensure that the predicted value of the model can accurately and timely reflect the real situation of the controlled object[13]. The parameters $\boldsymbol{a}_i = [a_i, b_{i1}, \cdots, b_{iN}]^{\mathrm{T}}$ are updated in real time.

2.2.2 Adaptive predictive PID

In order to prevent the deterioration of the system regulation effect due to the low prediction accuracy of the prediction model, the adaptive proportion coefficient $z(0 \leqslant z \leqslant 1)$ is introduced. When the prediction accuracy of the prediction model is high, the proportion coefficient z is large, and PID control is dominant. On the contrary, when the proportion coefficient z is taken as a small value, the controller becomes the traditional PID control.

According to the grey model, the predicted output value at time $k+h$ can be calculated. The predicted error can be expressed as

$$\hat{e}(k) = y_r(k) - \hat{y}(k+h)$$

The actual measurement error can be expressed as

$$\bar{e}(k) = y_r(k) - y(k)$$

The adaptive proportion coefficient z is introduced, the system error signal input to PID controller is

$$e(k) = z\hat{e}(k) + (1 - z)\bar{e}(k) \quad (15)$$

The parameter proportion coefficient z can be adjusted according to the prediction accuracy of the model.

The control signal increment can be expressed as

$$\Delta\eta(k) = Ae(k) - Be(k-1) + Ce(k-2)$$

$$A = K_p\left(1 + \frac{Z_s}{T_I} + \frac{T_d}{Z_s}\right) \quad (16)$$

$$B = K_p\left(1 + \frac{2T_d}{Z_s}\right), \quad C = K_p \frac{T_d}{Z_s}$$

where, Z_s is the sample time, K_p is the proportional gain, T_I is the integral time, T_d is differential time. The actual control signal load $\eta(k)$ at time k is

$$\eta(k) = \eta(k-1) + \Delta\eta(k) \quad (17)$$

$\eta(k-1)$ is the load ratio at time $k-1$.

2.2.3 PID parameter optimization based on PSO

The PID controller parameter optimization has always been the focus of scholars. The control performance depends on the choice of parameters K_p, T_I, T_d and Z_s. The particle swarm optimization (PSO) algorithm is a fast and efficient swarm intelligence algorithm, which can obtain the best values of parameters K_p, T_I, T_d and Z_s.

In the final stage of convergence of the traditional PSO algorithm, the algorithm falls into the local optimal value, which is caused by the decrease of particle swarm diversity, and the convergence efficiency is low because the particles are easily trapped in the poor search area and it is difficult to jump out. In this work, the standard particle position and speed update algorithm is improved as

$$V_i(k+1) = \omega(k) V_i(k) + c_1 r_1 (G_{best.\,i} - x_i(k)) + c_2(k) r_2 (P_{best.\,i} - x_i(k)) \quad (18)$$

$$x_i(k+1) = x_i(k) + V_i(k+1)$$

$$\omega(k) = \omega_{start} - (\omega_{start} - \omega_{end}) \left(\frac{k}{T_{\max}}\right)^2 \quad (19)$$

$$c_2(k) = \beta(k) c_2$$

where, $\omega(k)$ represents the inertia weight, ω_{start} is the initial weight, ω_{end} is the inertia weight when the iteration reaches the maximum number, $T_{\max}$ is the maximum number of iterations, c_1 and c_2 are positive constant parameters usually in the range of [0 2] called acceleration coefficients and known also as the cognitive and collective parameters, $\beta(k)$ is the adaptive descending factor of the optimal solution of individual history, and its value in the range of [0 1], r_1 and r_2 are random variables generated for each speed update between [0 1], $V_i(k)$ is the speed of the ith particle at each iteration k, $x_i(k)$ is the position of the ith particle at each iteration k. In order to prevent the particle from searching blindly, the position and speed of the particle are limited. At last $P_{best.\,i}$ denotes the local best position of the ith particle at each iteration k, and $G_{best.\,i}$ defines the global best position at each iteration k.

The PSO algorithm is used to optimize multivariable PID controller parameters $\boldsymbol{P}$.

$$\boldsymbol{P} = [K_{p1}, T_{I1}, T_{d1}, Z_{s1}, \cdots, K_{pN}, T_{IN}, T_{dN}, Z_{sN}]$$

The objective of parameter optimization is to find a group of optimized multivariable PID parameters, so

that the system response speed is faster, and the overshoot is smaller, the settling time is shorter. In this work, quadratic control indicators are adopted.

$$J = \boldsymbol{E}^{\mathrm{T}}(k)\boldsymbol{Q}\boldsymbol{E}(k) + \boldsymbol{\eta}^{\mathrm{T}}(k)\boldsymbol{R}\boldsymbol{\eta}(k) \tag{20}$$

where,

$$\boldsymbol{Q} = \mathrm{diag}\{\boldsymbol{q}_1, \boldsymbol{q}_2, \cdots, \boldsymbol{q}_N\},$$
$$\boldsymbol{R} = \mathrm{diag}\{\boldsymbol{r}_1, \boldsymbol{r}_2, \cdots, \boldsymbol{r}_N\},$$
$$\boldsymbol{E}(k) = [\boldsymbol{e}_1(k), \boldsymbol{e}_2(k), \cdots, \boldsymbol{e}_N(k)]^{\mathrm{T}},$$
$$\boldsymbol{\eta}(k) = [\boldsymbol{\eta}_1(k), \boldsymbol{\eta}_2(k), \cdots, \boldsymbol{\eta}_N(k)]^{\mathrm{T}}.$$

The fitness function is taken as $f = \min J$, the optimization objective is to minimize J.

3 Simulation

To verify the effectiveness of the adaptive predictive PID, the two-stage reciprocating compressor is taken as the research object. The simulations among internal model control (IMC), conventional PID control and APPID control are carried out. Based on the two-stage compressor in Ref. [10], the relationship model between load and buffer tank pressure is expressed as the following differential equations.

$$\begin{cases} \dfrac{\mathrm{d}p_1}{\mathrm{d}t} = 287\left[95.4\eta_1 - 10.6p_1^{0.8}p_0^{-0.8}\eta_1 - (53 - 5.88p_2^{0.8}p_1^{-0.8})p_2\eta_2p_0^{-1}\right] \\ \dfrac{\mathrm{d}p_2}{\mathrm{d}t} = 123\left[0.9 \times (53 + 5.88p_2^{0.8}p_1^{-0.8})p_2\eta_2p_0^{-1} - 2.914 \times 10^{-3}p_2\xi\right] \\ p_1 \geqslant p_0,\ p_2 \geqslant p_0 \end{cases} \tag{21}$$

where, p_1 and p_2 represent the pressure of the 1st- stage buffer tank (absolute pressure) and the pressure of the 2nd-stage buffer tank (absolute pressure), p_0 is the standard atmosphere. The parameters η_1 and η_2 represent the 1st-stage intake load ratio and 2nd-stage intake load respectively. $\xi(0 \leqslant \xi \leqslant 1)$ represents the exhaust valve opening coefficient of the secondary buffer tank.

For the flow control of the two-stage compressor, the distributed control scheme is adopted, that is, the 2nd-stage pressure controlled by the 1st-stage load, and the 1st-stage pressure controlled by the 2nd-stage load. The sampling time is fixed as 1s. The performance is best when the prediction step size of the 1st and 2nd stage of the APPID controllers are 2 and 15 after several times of trial and error. The PSO optimization method is used to optimize the parameters of PID controller and APPID controller. The parameters of PSO algorithm are set as follows. Population size 50, particle dimension 6, maximum number of iterations 20, inertial weight declines gradually from 0.9 to 0.3, acceleration $c_1 = 1.494$, $c_2 = 1.494$, and the optimized results are shown in Table 1.

Table 1 Optimized PID controller parameters

	T_{I1}	K_{p1}	T_{d1}	T_{I2}	K_{p2}	T_{d2}
PID	0.74	1.36	0.05	1.34	−1.8	0
APPID	0.37	0.27	0	0.57	−0.7	0.57

At $t = 0$ s, a 60 kPa positive step signal is applied to the 2nd-stage pressure setting value. At $t = 300$ s, 60 kPa positive step signal is applied to the 1st stage exhaust pressure set value. When $t = 500$ s, a square-wave disturbance signal with duration of 100 s and amplitude of 30 kPa is applied to the 2nd-stage pressure. The simulation results under different controller are shown in Fig. 5 and Fig. 6. As can be seen from the figures, APPID controller has a significant improvement over the traditional PID controller in controlling overshoot. Compared with internal model controller, there are significant advantages in settling time while maintaining no overshoot.

In order to further analyze and compare the advantages and disadvantages of different controllers, the control performance indicators in the time domain are summarized as shown in Table 2. It can be seen that PID controller has the shortest settling time, but large

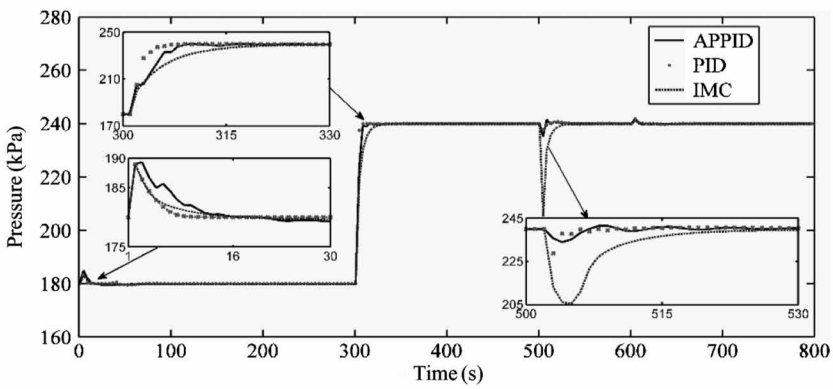

Fig. 5 The 1st stage pressure change trend diagram

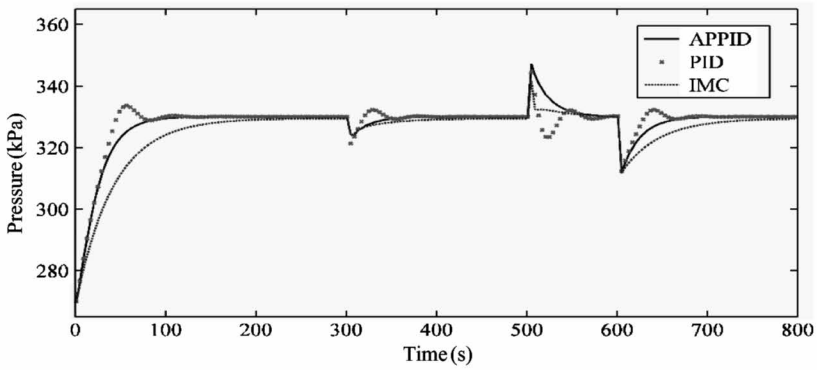

Fig. 6 The 2nd stage pressure change trend diagram

overshoot. The internal model controller has no overshoot, but the settling time is the longest and the control performance become poor when overcoming the fixed value disturbance. The advantage of the APPID controller is the integration of the internal model controller and the PID controller, which not only has no overshoot, but also a short settling time, while maintaining the ability of the PID controller to overcome the disturbance.

Table 2 Performance index of time domain control effect

	ISE	RT (s)	PT (s)	OT (%)	ST (s)	SE
IMC	230.8	130	0	0	120	0
Traditional PID	4.3769	45	12	7	108	0
APPID	1.204	65	0	0	55	0

RT: rise time; PT: peak time; OT: overshoot; ST: settling time; SE: steady error.

In order to further analyze the robustness, the opening coefficient of the exhaust valve is changed and the simulation is carried out under the original control parameters. The results are shown in Fig. 7 and Fig. 8. After the change of opening coefficient, the overshoot of PID controller increases. The internal model controller settling time increases, and in the case of a fixed value disturbance, oscillation and steady-state error occur. However, the APPID controller still has a high control performance. The results show that the APPID has a strong robustness after parameter optimization.

4 Application

The flow control scheme based on temperature and pressure ratio has been successfully applied to the flow regulation of air compressor and achieved good application effect.

There are 3 4M16 air compressors running in parallel in the air booster device of Sichuan Meifeng Chemical Co., Ltd. The rated exhaust flow of a compressor is 6 400 Nm^3/h, the rated power is 1.3 MW, and the speed is 375 rpm. Due to the change of gas consumption and ambient temperature, the exhaust flow of the device is large when 3 air compressors are running. However, the flow of the device is too small if only 2 compressors are running. In order to regulate the exhaust flow of the device, the 'one-back-one' backflow valve at the 1st stage of each compressor and the total vent valve are currently used, as shown in Fig. 9.

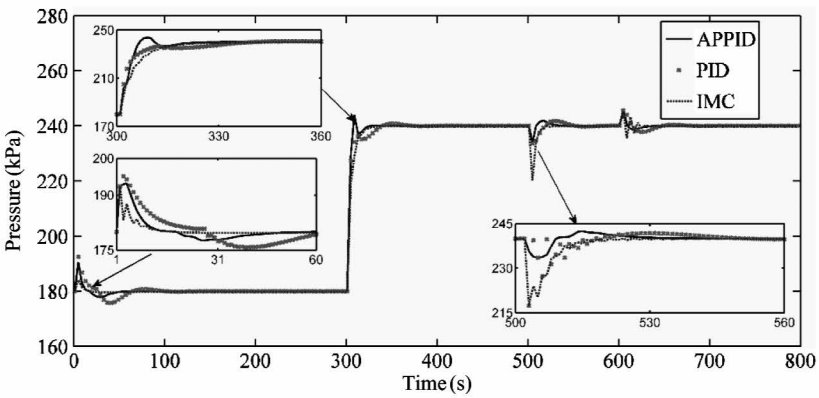

Fig. 7 Trend diagram of pressure change in the 1st stage when model mismatch

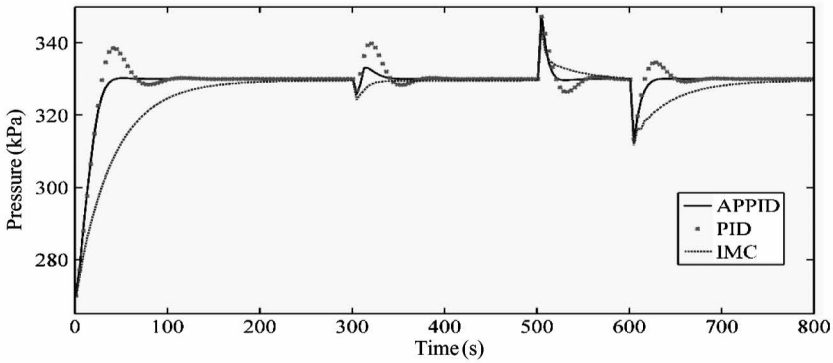

Fig. 8 Trend diagram of pressure change in the 2nd stage when model mismatch

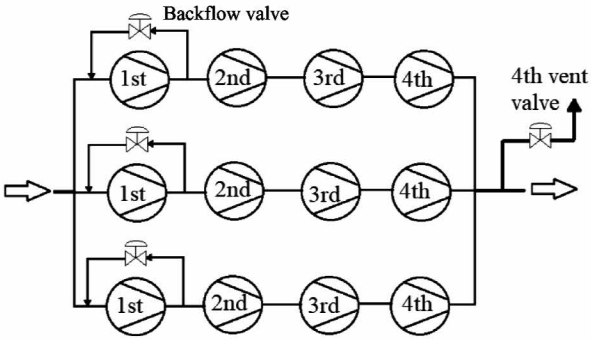

Fig. 9 Original exhaust flow control scheme

Although the structure is simple and can ensure smooth flow regulation of the device, it inevitably causes excessive power consumption of the 3 compressors. In order to solve the problem of energy waste caused by excessive exhaust, SCRS is added to the unit air compressor 103A. Its configuration scheme is shown in Fig. 10. The overall exhaust flow of the device is regulated by adjusting the exhaust flow of unit 103A, and the backflow valves of the other 2 compressors are closed. The control structure diagram is shown in Fig. 11.

The 1st stage load is calculated by the set exhaust flow and inlet temperature, while the 2nd stage, 3rd and 4th stage load are controlled in real time by APPID controller to ensure the pressure ratio of each stage of compressor.

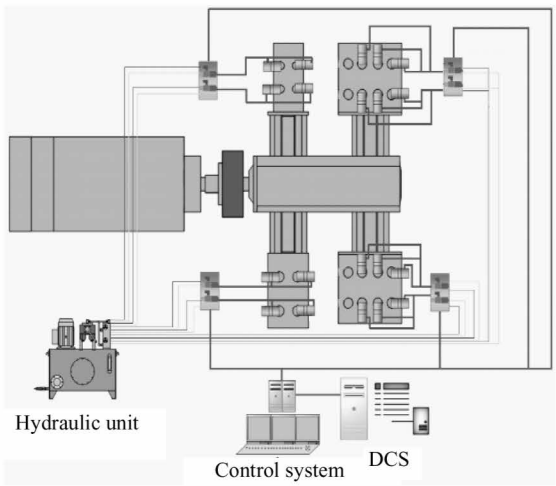

Fig. 10 Topology of capacity regulation system

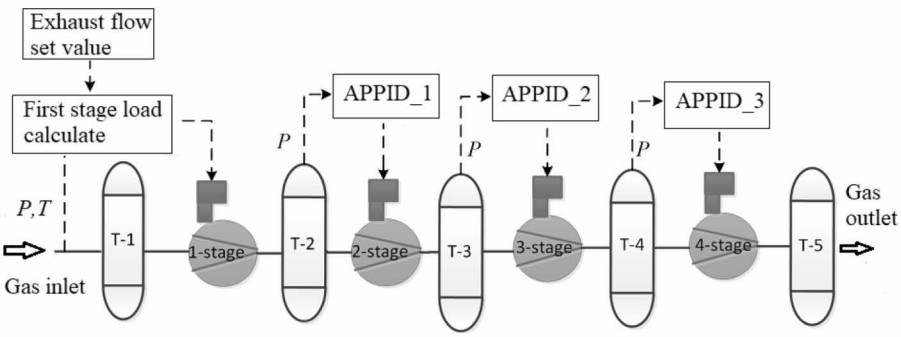

Fig. 11 System control flow chart

The temperature difference between day and night causes the change of compressor exhaust flow. The operating data of the system for consecutive 28 hours are analyzed, as shown in Fig. 12. It can be summarized that there is big difference in the inlet temperature between day (corresponding time period in Fig. 12 is 8 – 20 h) and night, with a maximum temperature of 22 ℃ and a minimum of 7 ℃. Based on the temperature and

pressure ratio flow control scheme, the 1st-stage load is adjusted according to the inlet temperature. The corresponding load is 66% at the minimum and 92% at the maximum. The APPID controller adjusts the load of other stages according to the set pressure ratio.

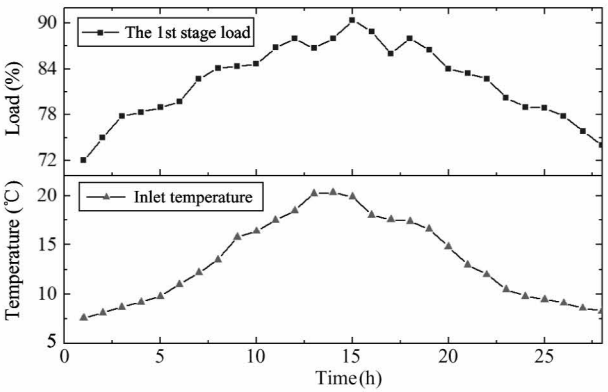

Fig. 12 The 1st stage load and inlet temperature

It can be seen from Fig. 13 that the exhaust flow also fluctuates in a small range near the set value of 16 850 Nm^3/h. The positive and negative deviations are 100 Nm^3/h and 200 Nm^3/h respectively.

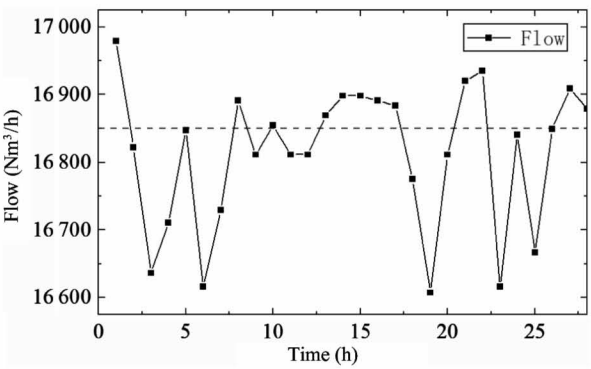

Fig. 13 Exhaust flow curve

Fig. 14 shows the effect of using APPID controller to control the compressor pressure ratio. The pressure of the first stage buffer tank is reduced from 120 kPa to 90 kPa, and there is no overshoot in the adjustment process. The adjustment time is 50 s. The pressure fluctuations of the 2nd and 3rd stage buffer tanks are 15 kPa and 34 kPa, respectively. When the pressure of the 2nd stage buffer tank increases from 400 kPa to 460 kPa, the adjustment time is 90 s without overshoot. The pressure fluctuation of the three-stage buffer tank is 20 kPa, while the pressure fluctuation of the 1st-stage buffer tank is less than 2 kPa. The pressure of the 3rd stage buffer tank increases from 1 000 kPa to 1 300 kPa, and there is also no overshoot in the adjustment process. The adjustment time is 75 s. During the adjustment process, the pressure of the 2nd stage buffer tank fluctuates by 6 kPa, while the first stage is not influenced. This shows that APPID can effectively overcome the influence of system delay on the adjustment performance and realize the pressure adjustment process without over-setting, and ensure the dynamic performance of the system.

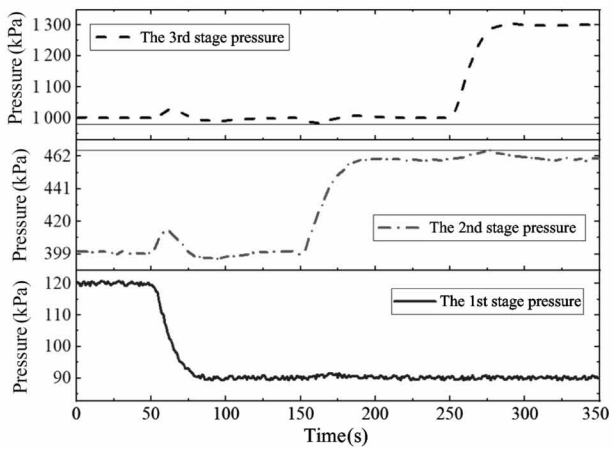

Fig. 14 Pressure ratio regulation process

When adjusting the pressure in the middle stage of the compressor, it is interesting to find that there is a large coupling effect on the rear stage, and then a small effect on the front stage, but almost no effect on the further front stage. Therefore, it can be considered that the coupling effect is unidirectional from front to back, while it is bidirectional between adjacent stages. Since the decoupling of each stage is not considered, changing the pressure of one stage has an effect on the other. The next work of this flow control scheme is to carry out decoupling among different stages.

To verify the energy saving effect of the system, the actual power comparison of different units under the same working condition is shown in Table 3. With the continuous reduction of the load, the power of the compressor 103A keeps decreasing, and the vent valve keeps turning down . The practical application results

Table 3 Power comparison between unit 103A and unit 102A

System pressure (MPa)	Load of 103A (%)	Power of 103A (MW)	Power of 102A (MW)	Valve opening (%)
2.70	100	1.21	1.12	58
2.71	85	1.10	1.12	48
2.70	70	1.02	1.09	43
2.71	50	0.92	1.11	39
2.70	45	0.88	1.09	33
2.70	40	0.82	1.12	20

show that the flow control scheme based on temperature and pressure ratio can realize the stable control of exhaust flow under the condition that the inlet temperature keeps changing, and the APPID controller can make the pressure ratio of each stage stable. Comparing the power of 2 compressor units, SCRS can save energy of the compressor and greatly reduce the energy waste of the compressor.

5 Conclusion

In this work, a novel flow control scheme based on inlet temperature and pressure ratio is proposed to solve the problem that the inlet temperature changes frequently, which results in the change of compressor's exhaust flow rate. The 1st stage load of the compressor is calculated through the set exhaust flow combined with the inlet temperature, and the pressure ratio of each stages are controlled by the APPID controller. Through the simulation model of two-stage reciprocating compressor, the performance of APPID is studied. Compared with the traditional PID and internal model control, APPID has more advantages in settling time, overshoot and robustness. Finally, the control scheme is applied to a four-stage air compressor in Sichuan Meifeng Chemical Industry Co., Ltd. By analyzing the operation data of a day when the temperature difference between day and night is more than 15 ℃, the effectiveness of the flow control scheme is verified. The 1st stage load of the compressor is automatically adjusted according to the inlet temperature, while the 2nd, 3rd and 4th stage load are adjusted by APPID controller to ensure stable pressure ratio. The power of the compressor is decreasing with the decrease of the compressor load, and the energy saving of the compressor is realized.

References

[1] Pichler K, Lughofer E, Pichler M, et al. Fault detection in reciprocating compressor valves under varying load conditions[J]. *Mechanical Systems and Signal Processing*, 2016, 70-71: 104-119

[2] Li D C, Wu H Q, Gao J J. Experimental study on stepless capacity regulation for reciprocating compressor based on novel rotary control valve[J]. *International Journal of Refrigeration*, 2013, 36(6):1701-1715

[3] Liu G B, Zhao Y Y, Tang B, el at. Dynamic performance of suction valve in stepless capacity regulation system for large-scale reciprocating compressor[J]. *Applied Thermal Engineering*, 2016, 96:167-177

[4] Tang B, Zhao Y Y, Li S, et al. Thermal performance analysis of reciprocating compressor with stepless capacity control system[J]. *Applied Thermal Engineering*, 2013, 54(2):380-386

[5] Chen J. Application of ISC capacity control system in reciprocating compressor[J]. *Petrochemical Automation*, 2014, 50(1):26-28

[6] Liu G B, Li Q Y, Cen Q S, et al. Study on dynamic process of suction valve in reciprocating compressor with capacity regulation system[J]. *Fluid Machinery*, 2015, 43(7):47-50

[7] Wang Y, Zhang J J, Zhou C, et al. A continuous capacity regulation system for a reciprocating compressor based on stage-by-stage recursive backflow control[J]. *Journal of Beijing University of Chemical Technology (Natural Science Edition)*, 2018,45(3):84-89

[8] Yang C J, Ma W, Han J C, el at. Application of DidroCom stepless gas control system in make up hydrogen compressor[J]. *Process Equipment and Piping*, 2019(1): 42-45

[9] Wang Z F, Lou D S, Feng W D, el at. HydroCOM gas capacity stepless regulating system for fresh hydrogen compressor in hydrocracking unit[J]. *Control and Instruments in Chemical Industry*, 2018(12):917-920

[10] Liu W H, Jiang Z N, Zhang T Y, et al. Optimization technology of capacity control method for reciprocating compressor[J]. *Control Engineering of China*, 2019,26(7):1365-1371

[11] Wu Y Z. Mathematical Model and Application of Reciprocating Compressor[M]. Xi'an: Xi'an Jiaotong University Press, 1989:165-168

[12] Wang Y, Jiang Z Z, Zhang J, el at. Performance analysis and optimization of reciprocating compressor with stepless capacity control system under variable load conditions[J]. *International Journal of Refrigeration*, 2018, 94: 174-185

[13] Yang C C, Zhang J G. Temperature of air-conditioning control based on grey predicative fuzzy PID control algorithm[J]. *Electronic Technology Application*, 2012, 38(4):56-59

Liu Wenhua, born in 1993. He is currently pursuing his Ph. D degree in Diagnosis and Self-recovery Engineering Research Center of Beijing University of Chemical Technology. His research interests include the design of stepless capacity regulation systems for reciprocating compressors and control algorithms for multivariable nonlinear systems.